http://dx.doi.org/10.5935/0103-5053.20150211

*J. Braz. Chem. Soc.*, Vol. 26, No. 11, 2249-2257, 2015.
Printed in Brazil - ©2015 Sociedade Brasileira de Química
0103 - 5053 $6.00+0.00

Article

# Removal of Lead(II), Copper(II) and Zinc(II) Ions from Aqueous Solutions Using Magnetic Amine-Functionalized Mesoporous Silica Nanocomposites

*Ali Mehdinia,*[,a] Sahar Shegefti[b] and Farzaneh Shemirani[b]*

[a]*Department of Marine Living Sciences, Marine Science Center, Iranian National Institute for Oceanography and Atmospheric Science, 14155-4781 Tehran, Iran*

[b]*Department of Analytical Chemistry, University College of Science, University of Tehran, 14155-6455 Tehran, Iran*

In this work, a batch adsorption study was conducted to investigate the removal efficiency of lead, copper and zinc ions from aqueous solutions. Magnetic amine-functionalized mesoporous silica nanoparticles were synthesized by grafting amine groups within the channels of magnetic mesoporous silica nanocomposites. Morphological and structural characterizations were made by X-ray powder diffraction, $N_2$ adsorption-desorption, scanning and transmission electron microscopy, Fourier transform infrared spectroscopy and elemental analysis. Among different factors influencing the sorption process, solution pH, shaking time and mass of adsorbent were investigated. The removal efficiencies were higher than 98% under optimized experimental conditions. Maximum adsorption capacities calculated by the Langmuir model were 268, 93 and 82 mg $g^{-1}$, for lead(II), copper(II) and zinc(II) ions, respectively. Accuracy and applicability of the synthesized adsorbent was estimated by analyzing spiked natural water samples and good recoveries (> 95%) were obtained with no matrix interferences.

**Keywords:** adsorption, amino-functionalization, toxic metal ion removal, magnetic nanocomposite, MCM-41

## Introduction

The removal of toxic metal ion contaminants from aqueous samples is one of the major economic and environmental problems all over the world.[1,2] Toxic metal ions, sometimes even at relatively low concentration, can cause serious hazardous effects on public health, due to their toxicity, carcinogenic effects and tendency to bioaccumulation in living tissues particularly in human bodies. They can cause significant physiological disorders such as damage to central nervous system and blood composition, production of energy and irreversible damage of vital organs of body.[3,4] Lead(II), copper(II) and zinc(II) are among the most common toxic metal ion pollutants which are released into the water environment due to the different industrial and natural processes.[1,5] The redistribution of toxic metal ions can adversely affect water resources and endanger the surrounding ecosystems and human health; therefore, the removal of toxic metal ions from waters and wastewaters is essential in terms of safety of public health and environment.[6] The conventional methods for removal of toxic metal ions from water and wastewater include oxidation, reduction, precipitation, membrane filtration, ion exchange and adsorption.[7] However, most available methods may show economical and technical disadvantages, such as high capital and operational costs, high sensitivity to operational conditions, significant energy consumption, handling and disposal problems, sludge generation and inefficient removal especially at low metal concentrations.[3,4,8]

Among these methods, adsorption-based methodology has been considered an attractive approach due to its simplicity, flexibility, cost-effectiveness (because of lower consumption of reagents) and environmental friendliness (especially in case of using adsorbents of natural origin). However, adsorbents with high adsorption capacity, fast adsorption-desorption kinetics and easy fixation and separation from water are in great demand.[2,5] There are many types of adsorbents, including natural materials (zeolites, clays and lignite), silica gel, activated carbon, oxide minerals, resins, polymeric hybrid sorbents, fibers, waste materials and biosorbents, which have been used

*e-mail: mehdinia@inio.ac.ir

to adsorb metal ions from aqueous solutions.[2,7] However, most adsorbents are nonselective and remove not only the target pollutants but also minerals present in water. This significantly decreases the capacity and life of the adsorbent for the target pollutants[9] while an ideal adsorbent should have features of strong affinity to target and large surface area with more binding sites. Thus, it necessitates the development of new adsorbents which have shown significant enhancement in toxic metal ion removal efficiencies from water.[10]

In the past several years, there has been an increasing interest in developing magnetic mesoporous particles, with enhanced textural properties that allow their use as adsorbents, catalysts or drug carriers.[11] Magnetic separation may become one of the promising methods for removal of pollutants in water because of generating no secondary waste and consequently producing no additional pollution, and also adapting with the complex separation conditions. Iron oxides are not mainly chosen due to their favorable magnetic properties, but also to their high availability, convenience of the preparation route and biocompatibility. Magnetite and maghemite have the highest saturation magnetizations among the iron oxides.[12] Additionally, the ordered mesoporous silica materials such as MCM-41 and SBA-15 are preferred due to their uniform pores with size in a range of 1.5-20 nm, high pore volume, unique large surface area, high sorption capacity and great diversity in surface functionalization in conjunction with high hydrothermal and chemical stability. So, they could be considered ideal coatings to protect the inner magnetic core.[13,14] Fellenz *et al.*[15] reported synthesis and magnetic characterization of magnetite particles embedded in mesoporous MCM-41. Jing-po *et al.*[16] reported Hg(II) sensing and removal performance of a core-shell structured nanocomposite. The inner core was composed of superparamagnetic $Fe_3O_4$ nanoparticles and the outer shell was composed of silica molecular sieve MCM-41. Bing[17] also reported a core-shell structured nanocomposite for Hg(II) sensing and removal, using superparamagnetic $Fe_3O_4$ nanodots as the core and silica molecular sieve MCM-41 as the shell. To further facilitate the adsorption affinity, surface modification has often been used. It has been reported that the amino-functionalized materials demonstrated outstanding ability to remove a wide variety of toxic metal ions from aqueous solutions owing to the strong metal complexing capability of amino groups. Regeneration of metal-loaded amino-functionalized adsorbents can be easily achieved by proton displacement of the metal ion with acid washing.[8] Chung *et al.*[18] reported sorption of lead(II) and copper(II) onto multi-amine grafted mesoporous silica embedded with nano-magnetite.

In this work, magnetic amine-functionalized mesoporous silica adsorbent ($Fe_3O_4$@MCM-41-$NH_2$) was synthesized by covalently grafting amino groups onto the inner surface of magnetic MCM-41. The adsorbent was characterized and the effect of experimental conditions on the removal efficiency of lead(II), copper(II) and zinc(II) ions from aqueous solution was investigated in batch mode and the isotherm equilibrium data were fitted to the Langmuir isotherm. Performance of the prepared material in removal of the toxic metal ions from natural water matrices with fast adsorption equilibrium was satisfying.

## Experimental

A Vista-MPX inductively coupled plasma optical emission spectrometry (ICP-OES, Varian Inc., Melbourne, Victoria 3170) equipped with a slurry nebulizer and a charge coupled device detector was used for determination of the analytes. Argon gas for ICP-OES with the purity of 99.999% was purchased from Roham Gas Company. The operational conditions and analytical wavelength of the metal ions were shown in Table 1.

**Table 1.** Instrumental parameters of ICP-OES and metal ion emission lines

| Parameter | Value |
|---|---|
| Radiofrequency generator power / kW | 1.3 |
| Plasma gas flow rate / (L $min^{-1}$) | 15 |
| Auxiliary gas flow rate / (L $min^{-1}$) | 1.5 |
| Nebulizer pressure / kPa | 150 |
| Torch mode | axial |
| Analytical lines / nm | $Pb^{2+}$ (220), $Cu^{2+}$ (327), $Zn^{2+}$ (213) |

The resulting adsorbent was characterized by scanning electron microscopy (SEM) VEGA TESCAN equipped with energy dispersive X-ray spectroscopy (EDX), transmission electron microscopy (Philips CM30 TEM), dynamic light scattering (DLS, Malvern, MAL1001767) and Fourier transform infrared spectroscopy (FTIR, Bruker VERTEX 70 spectrometer). X-ray powder diffraction (XRD) was performed on X'Pert pro MPD diffractometer equipped with a PIXel detector (PANalytical Company). The sample was scanned in step size 0.01°, time *per* step of 170 s, and the acquisition time of 15 min. The $N_2$ adsorption-desorption isotherm was determined using a Belsorp mini II (Japan Co.) at −196 °C; after that, the adsorbent was dehydrated and degassed at 120 °C for 13 h. The specific surface area was determined in relative pressure of 0.05-0.2, and cross-sectional area was also

0.162 $nm^2$. The surface area and the pore distribution were calculated by Brunauer-Emmett-Teller (BET) and Barret-Joyner-Halenda (BJH) equations.[19]

Iron(III) chloride hexahydrate ($FeCl_3.6H_2O$), iron(II) chloride tetrahydrate ($FeCl_2.4H_2O$), ammonium hydroxide ($NH_4OH$), cetyltrimethyl ammonium bromide (CTAB), sodium silicate, 3-aminopropyltriethoxysilane (APTES) and toluene were purchased from Merck. The lead(II), copper(II) and zinc(II) working solutions were prepared daily from their stock standard solutions (1000 mg $L^{-1}$) (Merck). Sodium hydroxide (NaOH) and nitric acid ($HNO_3$) 65% (Merck) were used for adjusting pH of the solutions.

For preparation of colloidal suspension magnetic nanoparticles, $FeCl_3.6H_2O$ (2 g) and $FeCl_2.4H_2O$ (0.8 g) were dissolved in 10 mL of distilled water and was added dropwise to a 100 mL solution of 1.0 mol $L^{-1}$ $NH_4OH$ solution containing 0.4 g of CTAB under nitrogen atmosphere while increasing the temperature up to 80 °C. The black solution was acquired and sonicated.

The resultant solution (20 mL) was added dropwise to 840 mL solution of distilled water containing 140 mL of $NH_4OH$ (1 mol $L^{-1}$) and 4 g of CTAB. Then 16 mL of sodium silicate was slowly added and maintained in a closed container under stirring for 24 h. The resulting magnetic MCM-41 was filtered and washed. The surfactant template was then removed from the synthesized material by calcination at 450 °C for 4 h.

After synthesis of magnetic MCM-41, 1.024 mL of APTES was added as an agent to modifying the surface of MCM-41 and the solution was refluxed with toluene under nitrogen atmosphere during 120 min for three times to prepare the $Fe_3O_4$@MCM-41-$NH_2$.

Batch adsorption is a simple technique commonly utilized to assess the adsorptive capacities of natural and synthetic sorbents. Beside its easy manipulation, it helps to bring out important information about the efficiency of a given sorbent to remove the studied solute in static conditions. Thus, it is widely used for environmental purposes.[20] In the present study, batch experiments were performed in 50 mL tubes containing 20 mL of metal ion solution at predetermined initial concentrations of lead(II), copper(II) and zinc(II). The solution pH was adjusted to the desired value by adding 0.1 mol $L^{-1}$ $HNO_3$ and 0.1 mol $L^{-1}$ NaOH prior to mixing with a weighed amount of the adsorbent. The tubes were shaken at room temperature using a mechanical shaker for different time intervals to reach equilibrium. Then the adsorbent was removed magnetically from the solution using a permanent hand-held magnet. The initial concentrations of metal ions ($Pb^{2+}$, $Cu^{2+}$ and $Zn^{2+}$) and those of remaining in aqueous solutions were determined by ICP-OES. All experiments were carried out in duplicate and the values reported are average of two readings. Blank samples were run in parallel on metal solutions without addition of the adsorbent, showing that the experimental procedure did not lead to any reduction of metal concentration and pH variations were unrelated to sorbent effects. The removal efficiency (RF) was calculated according to the following equation 1, where $C_0$ and $C_e$ are the initial and equilibrium concentrations of metal ions in mg $L^{-1}$, respectively.

$$RF(\%) = \frac{C_0 - C_e}{C_0} \times 100 \quad (1)$$

## Results and Discussion

### Characterization of the magnetic $NH_2$-MCM-41

The XRD pattern of the prepared magnetic MCM-41 is presented in Figure 1. The result showed relatively well defined XRD pattern for magnetic MCM-41 material, with one strong peak around 2.45 and two small peaks at 4.25 and 4.83 that were assigned to (100), (110), and (200) planes, respectively. Moreover, the fourth peak at 6.44 can be observed and indexed as (210) in the hexagonal system. The observed well-resolved diffraction peaks come from the typical MCM-41. The particle size was about 20.4 nm calculated by Scherrer equation using (100) peak. $N_2$ adsorption/desorption isotherms of magnetic $NH_2$-MCM-41 is illustrated in Figure 2.

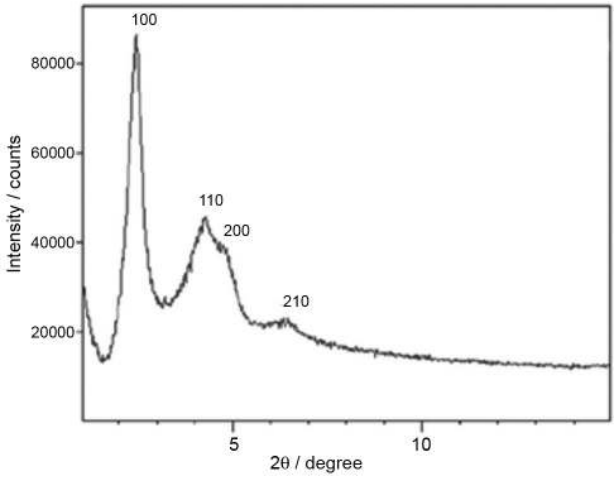


**Figure 1.**The XRD pattern of magnetic MCM-41.

It can be categorized as type IV curve, typical of the mesoporous materials. The inset shows the BJH pore size distribution of prepared adsorbent calculated from the desorption branch of the isotherm. The surface area and $r_{p,peak}$ of BJH plot that expressed mode of the

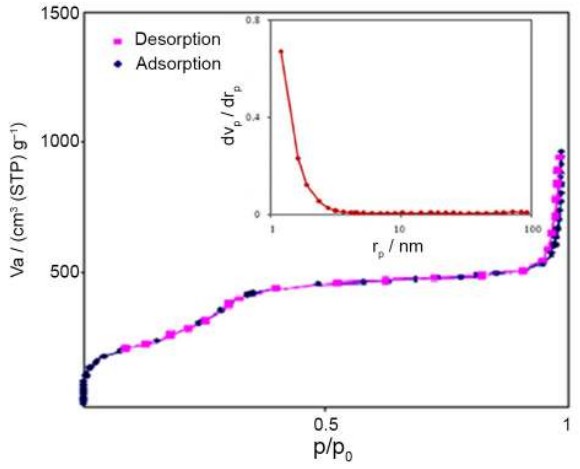


**Figure 2.** The $N_2$ adsorption-desorption isotherms of $Fe_3O_4$@MCM-41-$NH_2$ and the BJH plot of the prepared adsorbent (inset).

obtained pore radius in the structure of the synthesized $Fe_3O_4$@MCM-41-$NH_2$ were calculated to be 880 $m^2$ $g^{-1}$ and 1.8 nm, respectively.

FTIR analyses of magnetic MCM-41 and $NH_2$-MCM-41 are illustrated in Figures 3a and 3b. The peaks of 782, 958 and 1079 $cm^{-1}$ were attributed to Si-OH vibration, symmetric stretching and asymmetric stretching of Si–O–Si, respectively. In addition, the wide peak in region of 3000-3600 is related to OH stretching. The absorption bands at 500 to 600 $cm^{-1}$ usually attribute to the Fe–O stretches. Figure 3b also shows the symmetry and asymmetry stretching bonds of methyl group in the structure of modifier at the range of 2800-3000 $cm^{-1}$ which express amine functionalization of mesoporous substrate. In addition, the wide peak in the region of 3200-3400 $cm^{-1}$ could be related to NH stretching of amino groups.

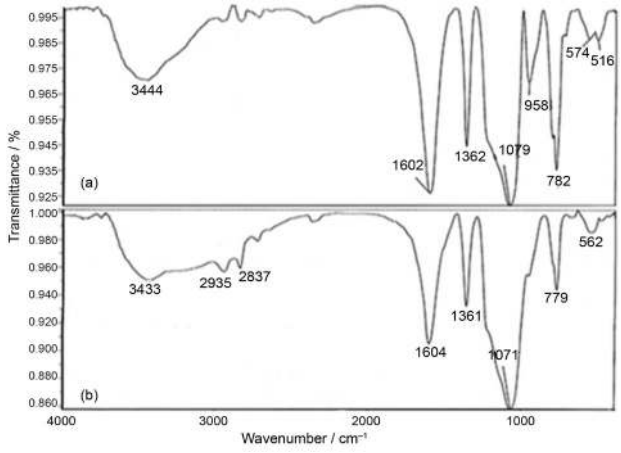


**Figure 3.** FTIR spectrums of magnetic (a) MCM-41; (b) $NH_2$-MCM-41.

Both SEM and TEM images (Figure 4) illustrate the spherical morphology for magnetic $NH_2$-MCM-41. Size estimation by DLS analysis proved that nanoparticles have

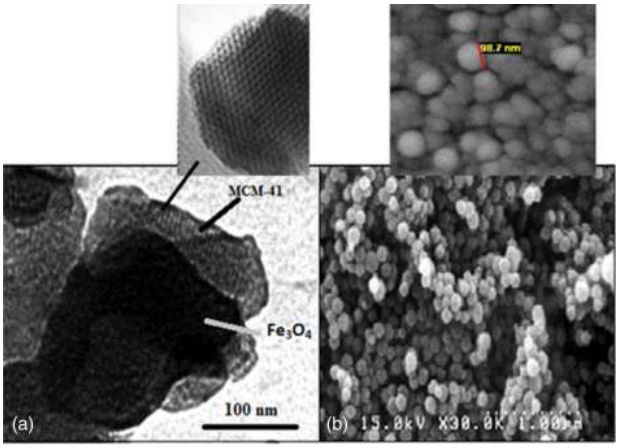


**Figure 4**. (a) TEM; (b) SEM images of $NH_2$-MCM-41 adsorbent.

diameters between 80-125 nm with the mean particle size of 105 nm.

Elemental analysis of the magnetic $NH_2$-MCM-41 using energy dispersive spectroscopy (EDS) was presented in Figure 5. The presence of Fe, O, N and Si elements confirms formation of the adsorbent.

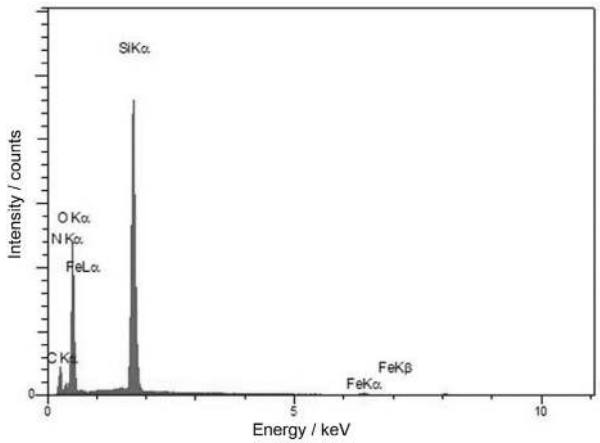


**Figure 5.** EDS image of magnetic $NH_2$-MCM-41.

## Effect of functionalization of adsorbent

For investigation of the functionalization effect on the removal efficiency of the adsorbent, a comparison was made between magnetic MCM-41and magnetic $NH_2$-MCM-41. The removal efficiencies of lead(II), copper(II) and zinc(II) ions reach from 62, 65 and 70% for magnetic MCM-41 to 88, 91 and 95% for magnetic $NH_2$-MCM-41, respectively. It can be seen in magnetic $NH_2$-MCM41, not only the regular porous structure of the silica substrate can adsorb the target analytes but also the presence of hydrophilic NH functional groups can cause a greater ability to remove the metal ions from the aqueous sample.

## Optimization

### Effect of pH

Earlier studies have indicated that solution pH is an important factor affecting adsorption of toxic metal ions onto the adsorbent. This may be because of the fact that pH influences both the chemistry of metal ions and surface functional groups.[9,21,22] Removal of lead(II), copper(II) and zinc(II) was studied as a function of pH within a pH range of 2.0-6.0 for lead(II) and 2.0-8.0 for copper(II) and zinc(II).

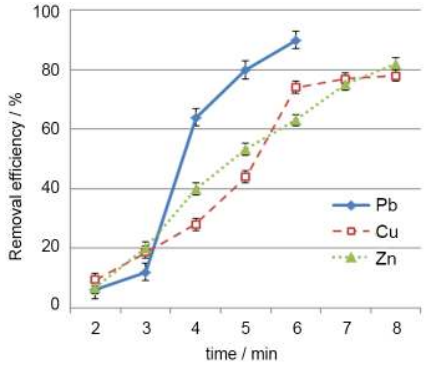


**Figure 6**. Effects of solution pH on removal of $Pb^{2+}$, $Cu^{2+}$ and $Zn^{2+}$ ions by $Fe_3O_4$@MCM-41-$NH_2$.

The other parameters including sample volume (20 mL), initial metal ion concentration (25 mg $L^{-1}$ for $Pb^{2+}$, 7.5 mg $L^{-1}$ for $Cu^{2+}$ and 1.5 mg $L^{-1}$ for $Zn^{2+}$), adsorbent dosage (5 mg) and shaking time (10 min) were maintained constant. The results were shown in Figure 6. Higher pH values were neglected to avoid the formation of metal hydroxide precipitates, which competes with the metal ions for the active sites on the adsorbent leading to the reduction in the retention of metal ions.[22] As it can be seen from this figure, the removal efficiencies of $Pb^{2+}$, $Cu^{2+}$ and $Zn^{2+}$ increased as pH was raised. Such phenomenon reveals the characteristic of chelation mechanism.[8] At low pH values, the adsorbent showed very low tendency for uptaking all the investigated metal ions due to protonation of its functional groups ($NH_3^+$) or competition of $H_3O^+$ with metal ions, which prevented approaching of the metal ions to the binding sites on the adsorbent. As the pH increased, more binding sites were released and the positive surface charge on the adsorbent decreased. It results in a lower electrostatic repulsion between the surface and the metal ions and hence, better adsorption behavior.[1,21] The removal efficiencies reached to 90% at pH of 6.0 for $Pb^{2+}$, 88% at pH of 7.0 for $Cu^{2+}$ and 87% at pH of 7.0 for $Zn^{2+}$.

### Effect of adsorbent dosage

The effect of adsorbent dosage on the removal efficiency of lead, copper and zinc were investigated under optimum pH by using different adsorbent values (5, 10, 12.5, 15 and 20 mg), while other parameters including sample volume (20 mL), initial metal ion concentrations (25 mg $L^{-1}$ for $Pb^{2+}$, 7.5 mg $L^{-1}$ for $Cu^{2+}$ and 1.5 mg $L^{-1}$ for $Zn^{2+}$) and shaking time (10 min) were maintained constant. It was observed (Figure 7) the percentage of removal increased in adsorbent dosage of 12.5 and 15 mg for $Cu^{2+}$ and $Zn^{2+}$, and $Pb^{2+}$ respectively, and the removal efficiencies were remained constant more or less at higher dosage of adsorbents. Therefore, 15 mg was selected for all studied metal ions.

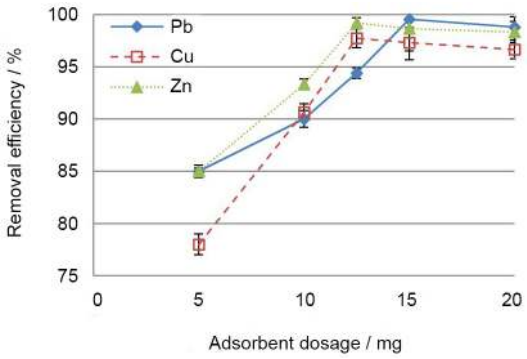


**Figure 7.** Effects of adsorbent dosage on removal of $Pb^{2+}$, $Cu^{2+}$ and $Zn^{2+}$ ions by $Fe_3O_4$@MCM-41- $NH_2$.

### Effect of shaking time

The importance of shaking time comes from the need to identify the possible rapidness of binding and removal processes of the investigated metal ions by the synthesized adsorbents and to obtain the optimum time for complete removal of the target metal ions.[22] Adsorption of $Pb^{2+}$, $Cu^{2+}$ and $Zn^{2+}$ onto $Fe_3O_4$@MCM-41-$NH_2$ at different shaking times (2, 5, 10 and 15 min) was studied at optimum solution pH and adsorbent dosage. The results were presented in Figure 8. The results showed that shaking time of 5 min was enough for complete removal of metal ions from 20 mL solution with concentration of 25, 7.5 and 1.5 mg $L^{-1}$ for $Pb^{2+}$, $Cu^{2+}$ and $Zn^{2+}$, respectively. Therefore, the optimum shaking

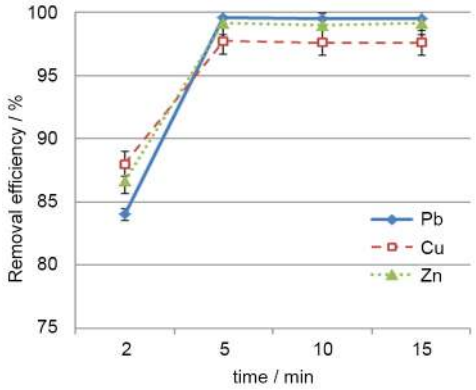


**Figure 8.** Effects of shaking time on removal of $Pb^{2+}$, $Cu^{2+}$ and $Zn^{2+}$ ions by $Fe_3O_4$@ MCM-41-$NH_2$.

time was considered to be 5 min. This fast adsorption rate that attributed to large external surface and high metal sorption capacity of adsorbent, suggests high adsorption efficiency and applicability for different applications.

### Adsorption isotherm

The relationship between the amount of a substance adsorbed *per* unit mass of adsorbent at constant temperature and its concentration in the equilibrium solution is called the adsorption isotherm. There are several well-known isotherm equations that are mainly employed to evaluate the adsorption capacity of an adsorbent for an adsorbate. Since the more common models are Freundlich and Langmuir equations, the experimental results were modeled using these in order to obtain the best fit isotherm. The Freundlich model is based on using an empirical equation that adopts multilayer adsorption on heterogeneous surfaces considering interaction between the adsorbed species.[3,4,8,23] The Freundlich isotherm is described by equation 2 and the linearized form of this model is represented by equation 3:

$$q_e = K_F C_e^{1/n} \quad (2)$$

$$\log q_e = \log K_F + \frac{1}{n} \log C_e \quad (3)$$

where $q_e$ and $C_e$ are the amount of metal ion adsorbed on the sorbent surface at equilibrium and the equilibrium metal ion concentration in the solution, respectively. Also, $K_F$ and n are the Frendlich constants related to the adsorption capacity and the adsorption intensity, respectively. They can be obtained from the intercept and the slope of linear plot of log $q_e$ *vs.* log $C_e$.

In the Langmuir model, it is assumed that the maximum adsorption corresponds to a saturated monolayer of solute molecules onto a surface containing a finite number of uniform and energetically equivalent adsorption sites, with no subsequent interaction among adsorbed molecules and no transition in the plane of surface.[2,24] The expression of the Langmuir model and the linearized form of it are given by equations 4 and 5, respectively,

$$q_e = \frac{b\, q_{max} C_e}{1 + b\, C_e} \quad (4)$$

$$\frac{1}{q_e} = \frac{1}{q_{max}} + \frac{1}{q_{max} b} \cdot \frac{1}{C_e} \quad (5)$$

where $q_e$ and $C_e$ are the same as in equation 2. Also, $q_{max}$ and b are the Langmuir constants, representing the maximum adsorption capacity and the energy constant related to the heat of adsorption, respectively.

The adsorption studies were conducted by varying the initial metal ion concentrations with a constant dosage of adsorbent, optimum pH and shaking time of 5 min. The Langmuir and Freundlich isotherms were shown graphically in Figure 9 and the corresponding parameters were presented in Table 2. According to the coefficients of correlation obtained from linear regression, it was found that in all cases the Langmuir model fit the data better than the Freundlich model.

The maximum adsorption capacities calculated from the Langmuir model were 268, 93 and 82 mg $g^{-1}$ which agreed

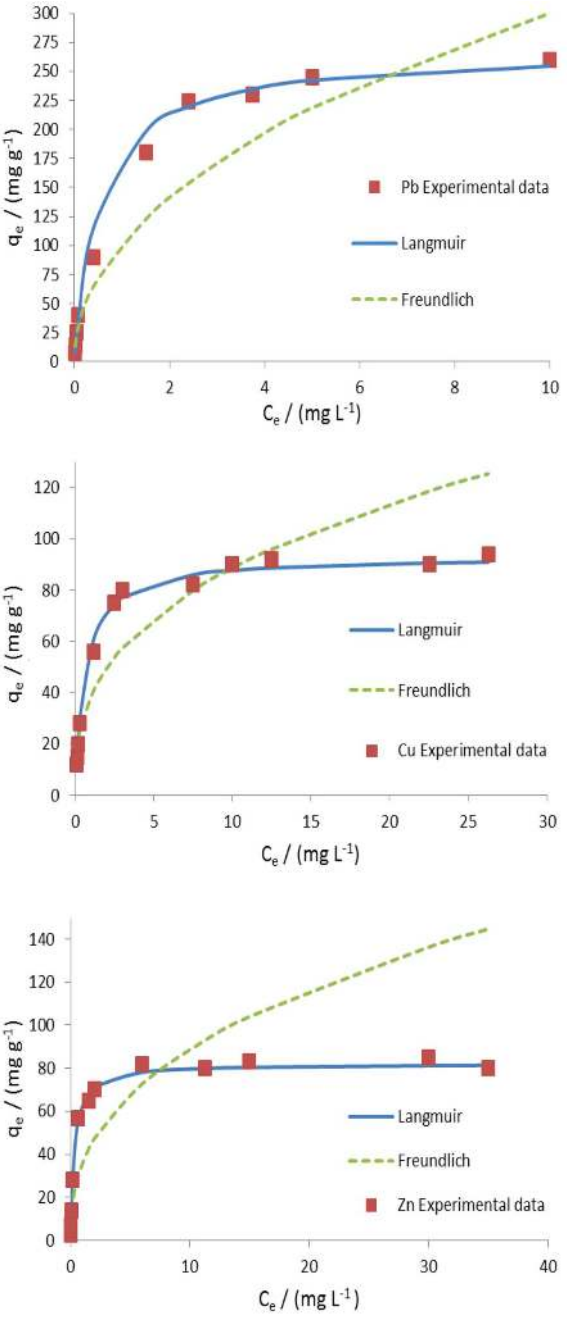


**Figure 9.** Adsorption isotherms of $Pb^{2+}$, $Cu^{2+}$ and $Zn^{2+}$.

**Table 2.** Freundlich and Langmuir constants

| | $Pb^{2+}$ | $Cu^{2+}$ | $Zn^{2+}$ |
|---|---|---|---|
| Langmuir | | | |
| $q_{max}$[a] / (mg $g^{-1}$) | 268 | 93 | 82 |
| b[b] / (l $mg^{-1}$) | 1.98 | 1.62 | 3.33 |
| $R^2$[c] / % | 99.7 | 98.8 | 99.4 |
| Freundlich | | | |
| $K_F$[d] / (mg $^{1-1/n}$ L $^{1/n}$ $g^{-1}$) | 106.6 | 38.6 | 36.2 |
| 1/n[e] | 0.50 | 0.36 | 0.39 |
| $R^2$[c] / % | 94.1 | 90.9 | 84.9 |

[a]$q_{max}$: Langmuir constant representing the maximum adsorption capacity; [b]b: Langmuir constant representing the energy constant related to the heat of adsorption; [c]$R^2$: coefficient of determination; [d]$K_F$: Frendlich constant related to the adsorption capacity; [e]n: Frendlich constant related to the adsorption intensity.

very well with their experimental values. Comparative information on removal of $Pb^{2+}$, $Cu^{2+}$ and $Zn^{2+}$ with those of other published results is given in Table 3. The comparative results show that the removal efficiencies of the prepared adsorbent were comparable or higher, in some cases, than the most reported adsorbents in Table 3. Moreover, it was noted that the contact time required for the metal adsorption using this adsorbent was short and the adsorption equilibriums were reached within few minutes for ionic species examined.

The higher selectivity of the proposed adsorbent to the toxic metal ions than the other cations in water samples may be explained by the complexation capability (donor-acceptor interaction) of the -$NH_2$ groups on the surface of the adsorbent and toxic metal ions such as $Zn^{2+}$, $Cu^{2+}$ and $Pb^{2+}$.

**Table 3.** Comparison of $Pb^{2+}$, $Cu^{2+}$ and $Zn^{2+}$ adsorption on $Fe_3O_4$@ MCM-41-$NH_2$ with other absorbents

| Metal | Adsorbent | Adsorption capacity / (mg $g^{-1}$) | Contact time / min | Removal efficiency / % | Reference |
|---|---|---|---|---|---|
| $Pb^{2+}$ | activated carbon from Ceibapentandra hulls | 25.5 | 50 | 99.5 | 1 |
| | $SiO_2$-nanoparticles-immobilized-Penicillium funiculosum | 262.5 | 20 | – | 3 |
| | magnetic porous ferrospinel $MnFe_2O_4$ | 69.1 | 180 | 96.7 | 5 |
| | amino-functionalized $Fe_3O_4$ | 40.1 | – | 98.0 | 8 |
| | polymer-supported nanosized hydrous manganese dioxide | 395.0 | – | – | 10 |
| | magnetic alginate beads | 100.0 | 100 | – | 12 |
| | EDTA-modified mesoporous silica SBA-15 | 273.2 | 20 | 92.0 | 13 |
| | silica gel/chitosan composite | 316.0 | 15 | – | 14 |
| | PANI/MWCNTs | 22.2 | – | 90.0 | 25 |
| | $Fe_3O_4$@APS@AA-co-CA | 166.1 | 45 | – | 26 |
| | EDTA-modified chitosan/$SiO_2$/$Fe_3O_4$ | 12.5 | 180 | 97.0 | 27 |
| | SH-mSi@$Fe_3O_4$ | 91.5 | – | – | 28 |
| | $Fe_3O_4$/cyclodextrin polymer nanocomposites | 64.5 | 45 | 99.5 | 29 |
| | $Fe_3O_4$@ MCM-41-$NH_2$ | 268.0 | 5 | 99.7 | present work |
| $Cu^{2+}$ | magnetic porous ferrospinel $MnFe_2O_4$ | 37.6 | 180 | 97.8 | 5 |
| | silica gel/chitosan composite | 870.0 | 15 | – | 14 |
| | $Fe_3O_4$@APS@AA-co-CA | 126.9 | 45 | – | 26 |
| | EDTA-modified chitosan/$SiO_2$/$Fe_3O_4$ | 44.4 | 360 | 98.6 | 27 |
| | PAA-coated $Fe_3O_4$ | 12.4 | – | 100.0 | 30 |
| | 1,6-hexadiamine-$Fe_3O_4$ | 25.8 | 5 | 98.0 | 31 |
| | EDTA functionalized silica | 79.4 | 60 | – | 32 |
| | diamine modified mesoporous silica on MWCNTs | 66.6 | 180 | – | 33 |
| | $Fe_3O_4$@ MCM-41-$NH_2$ | 93.0 | 5 | 98.8 | present work |
| $Zn^{2+}$ | activated carbon from Ceibapentandra hulls | 24.1 | 50 | 99.1 | 1 |
| | $Fe_3O_4$@APS@AA-co-CA | 43.4 | 45 | – | 26 |
| | EDTA functionalized silica | 74.1 | 60 | – | 32 |
| | $Fe_3O_4$@MCM-41-$NH_2$ | 82.0 | 5 | 99.4 | present work |

**Table 4.** Determination of $Pb^{2+}$, $Cu^{2+}$ and $Zn^{2+}$ in water samples

| Matrix | $Pb^{2+}$ | | $Cu^{2+}$ | | $Zn^{2+}$ | |
|---|---|---|---|---|---|---|
| | Spiked / (mg $L^{-1}$) | Recovery / % | Spiked / (mg $L^{-1}$) | Recovery / % | Spiked / (mg $L^{-1}$) | Recovery / % |
| Ground Water | 10 | 96 | 5 | 97 | 1 | 98 |
| Tap water | 5 | 95 | 2 | 96 | 0.5 | 97 |
| River water | 5 | 96 | 2 | 95 | 0.5 | 97 |

### Desorption and reuse

In addition to excellent adsorption capacity, it was highly desirable that an adsorbent could be reused repeatedly regarding the cost.[13] The pH study suggested that desorption of $Pb^{2+}$, $Cu^{2+}$ and $Zn^{2+}$ from $Fe_3O_4$@MCM-41-$NH_2$ was possible around pH 2, because under acidic conditions the adsorbent surface is protonated by $H_3O^+$ ions to make possible desorption of positively charged metal ions from its surface. Therefore, acid treatment (with 0.1 mol $L^{-1}$ $HNO_3$) was used for this purpose. In order to show the reusability of the adsorbent an adsorption/desorption cycle was repeated five times. As shown in Figure 10, the removal efficiency of the $Fe_3O_4$@MCM-41-$NH_2$ after three cycles was higher than 85%.

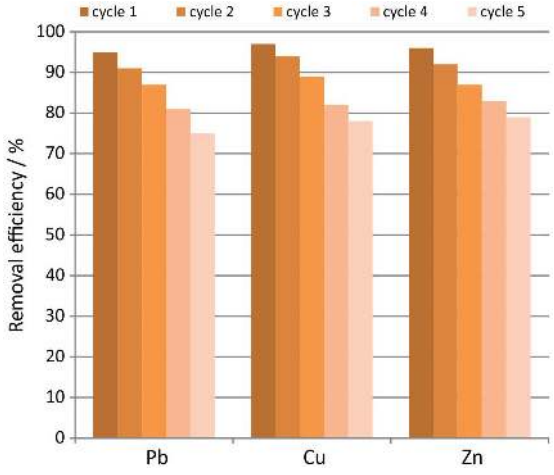


**Figure 10.** Removal efficiency of $Pb^{2+}$, $Cu^{2+}$ and $Zn^{2+}$ *versus* number of reuse cycles.

### Real sample analysis

For accessing the capability of magnetic $NH_2$-MCM-41 for removal of lead, copper and zinc ions from different natural water samples, the method was applied to different spiked water samples including ground, tap and river waters. The data obtained are presented in Table 4. It was found that prepared adsorbent showed good recoveries for $Pb^{2+}$, $Cu^{2+}$ and $Zn^{2+}$ in different natural water resources, with removal efficiencies of over 95%.

## Conclusions

In the present paper, the synthesis of $Fe_3O_4$@MCM-41-$NH_2$ was reported. The study indicated that magnetic MCM-41-$NH_2$ could be used as an effective adsorbent material for removal of lead, copper and zinc ions from water sample with a minimum contact time of 5 min. The adsorption of these toxic metal ions on adsorbent was dependent on contact time, pH and dose of the adsorbent. The equilibrium data was well fitted with Langmuir adsorption isotherm which showed an efficient adsorption of lead(II), copper(II) and zinc(II) ions due to the amine groups of the adsorbent. The regeneration of adsorbent was achieved using 0.1 mol $L^{-1}$ $HNO_3$ and it can be reused in three successive adsorption-regeneration cycles. Therefore, the amino-functionalized magnetic MCM-41 could be regarded as a potential candidate for high efficient and renewable adsorbent of lead(II), copper(II) and zinc(II) ions.

## Acknowledgments

The Iranian National Science Foundation is acknowledged for financial supporting the work.

## References

1. Rao, M. M.; Chandra Rao, G. P.; Seshaiah, K.; Choudary, N. V.; Wang, M. C.; *Waste Manage.* **2008**, *28,* 849.
2. Albishri, H. M.; Marwani, H. M.; Batterjee, M. G.; Soliman, E. M.; *Arab. J. Chem.* **2013**, *in press*, DOI:10.1016/j.arabjc.2013.07.023.
3. Mahmoud, M. E.; Yakout, A. A.; Abdel-Aal, H.; Osman, M. M.; *Bioresour. Technol.* **2012**, *106*, 125.
4. Farghali, A. A.; Bahgat, M.; Enaiet Allah, A.; Khedr, M. H.; *Beni-Suef Univ. J. Basic Appl. Sci.* **2013**, *2 (2)*, 61.
5. Ren, Y.; Li, N.; Feng, J.; Luan, T.; Wen, Q.; Li, Z.; Zhang, M.; *J. Colloid Interface Sci.* **2012**, *367*, 415.
6. Sahu, M. K.; Mandal, S.; Dash, S. S.; Badhai, P.; Patel, R. K.; *J. Environ. Chem. Eng.* **2013**, *1 (4)*, 1315.
7. Jin, G. P.; Zhu, X. H.; Li, C. Y.; Fu, Y.; Guan, J. X.; Wu, X. P.; *J. Environ. Chem. Eng.* **2013**, *1 (4)*, 736.

8. Tan, Y.; Chen, M.; Hao, Y.; *Chem. Eng. J.* **2012**, *191*, 104.
9. Chen, X.; Chen, G.; Chen, L.; Chen, Y.; Lehmann, J.; McBride, M. B.; Hay, A. G.; *Bioresour. Technol*. **2011**, *102*, 8877.
10. Su, Q.; Pan, B.; Pan, B.; Zhang, Q.; Zhang, W.; Lv, L.; Wang, X.; *Sci. Total Environ*. **2009**, *407*, 5471.
11. Morales, M. A.; Mascarenhas, A. J. S.; Gomes, A. M. S.; Leite, C. A. P.; Andrade, H. M. C.; de Castilho, C. M. C.; Galembeck, F.; *J. Colloid Interface Sci*. **2010**, *342*, 269.
12. Bée, A.; Talbot, D.; Abramson, S.; Dupuis, V.; *J. Colloid Interface Sci*. **2011**, *362*, 486.
13. Huang, J.; Ye, M.; Qu, Y.; Chu, Y.; Chen, R.; He, Q.; Xu, D.; *J. Colloid Interface Sci*. **2012**, *385*, 137.
14. Rajiv Gandhi, M.; Meenakshi, S.; *Int. J. Biol. Macromol.* **2012**, *50*, 650.
15. Fellenz, N. A.; Marchetti, S. G.; Bengoa, J. F.; Mercader, R. C.; Stewart S. J.; *J. Magn. Magn. Mater.* **2006**, *306*, 30.
16. Jing-po, Y.; Fei, L.; Jing, C.; Jin-di, Y.; *Microporous Mesoporous Mater.* **2015**, *202*, 175.
17. Bing, K.; *Sens. Actuators, B* **2014**, *198*, 342.
18. Chung, J.; Chun, J.; Lee, J.; Lee, S. H.; Lee, Y. J.; Hong, S.W.; *J. Hazard. Mater.* **2012**, *239-240*, 183.
19. Brunnauer, S.; Emmet, P. H.; Teller, E.; *J. Am. Chem. Soc*.**1938**, *60 (2)*, 309.
20. Sdiri, A.; Higashi, T.; Hatta, T.; Jamoussi, F.; Tase, N.; *Chem. Eng. J.* **2011**, *172*, 37.
21. Soliman, E. M.; Ahmed, S. A.; Fadl, A. A.; *Arab. J. Chem*. **2011**, *4*, 63.
22. Meitei, M. D.; Prasad, M. N. V.; *J. Environ. Chem. Eng.* **2013**, *1*, 200.
23. Giraldo, L.; Erto, A.; Moreno-Pirajan, J. C.; *Adsorption* **2013**, *19*, 465.
24. Olu-Owolabi, B. I.; Diagboya, P. N.; Ebaddan, W. C.; *Chem. Eng. J*. **2012**, *195-196*, 270.
25. Shao, D.; Chen, C.; Wang, X.; *Chem. Eng. J*. **2012**, *185-186*, 144.
26. Ge, F.; Li, M. M.; Ye, H.; Zhao, B. X.; *J. Hazard. Mater.* **2012**, *211-212*, 366.
27. Ren, Y.; Abbood, H. A.; He, F.; Peng, H.; Huang, K.; *Chem. Eng. J*. **2013**, *226*, 300.
28. Li, G.; Zhao, Z.; Liu, J.; Jiang, G.; *J. Hazard. Mater*. **2011**, *192*, 277.
29. Badruddoza, A. Z. M.; Shawon, Z. B. Z.; Daniel, T. W. J.; Hidajat, K.; Uddin, M. S.; *Carbohydr. Polym*. **2013**, *91*, 322.
30. Huang, S. H.; Chen, D. H.; *J. Hazard. Mater*. **2009**, *163*, 174.
31. Hao, Y. M.; Chen, M.; Hu, Z. B.; *J. Hazard. Mater*. **2010**, *184*, 392.
32. Kumar, R.; Barakat, M. A.; Daza, Y. A.; Woodcock, H. L.; Kuhn, J. N.; *J. Colloid Interface Sci.* **2013**, *408*, 200.
33. Yang, W.; Ding, P.; Zhou, L.; Yu, J.; Chen, X.; Jiao, F.; *Appl. Surf. Sci.* **2013**, *282*, 38.


*Submitted: March 28, 2015*
*Published online: August 25, 2015*